



# On the optical constants of amorphous $\text{Ge}_x\text{Se}_{1-x}$ thin films of non-uniform thickness prepared by plasma-enhanced chemical vapour deposition

E Márquez<sup>a,\*</sup>, P Nagels<sup>b</sup>, J M González-Leal<sup>a</sup>, A M Bernal-Oliva<sup>a</sup>, E Sleenckx<sup>b</sup>, R Callaerts<sup>b</sup>

<sup>a</sup>*Dpto. de Física de la Materia Condensada, Universidad de Cádiz, 11510, Puerto Real Cádiz, Spain*

<sup>b</sup>*RUCA, University of Antwerp, B-2020, Antwerpen, Belgium*

---

## Abstract

The preparation of layers of amorphous  $\text{Ge}_x\text{Se}_{1-x}$  (with Ge atomic concentrations  $x = 0, 0.17, 0.25$  and  $0.34$ ) by plasma-enhanced chemical vapour deposition (PECVD) using the hydrides,  $\text{GeH}_4$  and  $\text{H}_2\text{Se}$ , as precursor gases is described in detail. Information concerning the structure of the films was obtained from Raman spectroscopy. The optical transmission was measured over the 300 to 2500 nm spectral region in order to derive the refractive index and extinction coefficient of these PECVD films. The expressions proposed by Swanepoel, enabling the calculation of the optical constants of a thin film with non-uniform thickness, have successfully been applied. The refractive-index dispersion data were analysed using the Wemple–DiDomenico single-oscillator fit. The optical-absorption edges have been all of them described using the ‘non-direct transition’ model proposed by Tauc. The optical gaps were calculated using Tauc’s extrapolation, resulting in values ranging from 1.93 eV for  $a\text{-Se}$  to 2.26 eV for  $a\text{-GeSe}_2$ . © 1998 Elsevier Science Ltd. All rights reserved.

---

## 1. Introduction

Chalcogenide glasses of Ge–Se alloys are very interesting materials for infrared optics. They have a large range of transparency from around 0.6 to 30  $\mu\text{m}$  and good mechanical and chemical properties, such as hardness, adhesion, low internal stress and water resistance. Optical properties of the  $\text{Ge}_x\text{Se}_{1-x}$  system were reported by many authors for bulk glasses [1, 2] (which can be prepared only for  $x < 0.43$ ), for films prepared by evaporation [3–5], and for sputtered films [6, 7]. On the other hand, while plasma-enhanced chemical vapour deposition (PECVD) has become the preferred method of preparing amorphous silicon-type films, it has had considerably less impact on the preparation of chalcogenide layers. After some initial investigations by Fritzsche et al [8] failed to show significant differences between PECVD and thermally-

evaporated films for the As–S and As–Se systems, interest picked up again more recently, mainly after the works of Nagels et al [9, 10] and Cardinaud et al [11], when also Ge–Se layers were produced. In this paper, we report jointly on the optical constants and structure of amorphous Se-rich  $\text{Ge}_x\text{Se}_{1-x}$  films (i.e., with  $x \leq 0.34$ ) prepared by PECVD. It should be obviously emphasized that measurements of the variation in the properties of amorphous binary alloy semiconductors as a function of composition are very valuable from the viewpoint of tailoring materials with specific parameters.

## 2. Experimental procedure

### 2.1. Material preparation

We have deposited thin films of amorphous  $\text{Ge}_x\text{Se}_{1-x}$  (1 to 4  $\mu\text{m}$  thick and with Ge atomic concentrations  $x = 0, 0.17, 0.25$  and  $0.34$ ) in a plasma dis-

---

\* Corresponding author. Tel: +34 56 830966; Fax: +34 56 834924; e-mail: marquez@uca.es.

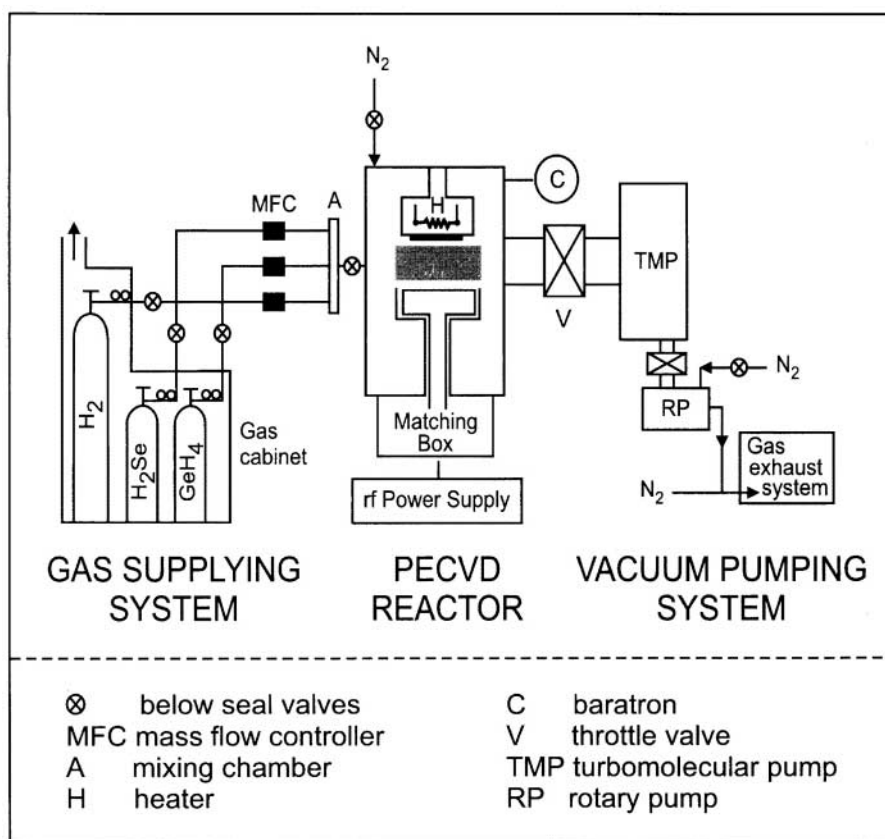


Fig. 1. Experimental arrangement used for plasma-enhanced CVD of amorphous chalcogenide layers.

charge stainless steel reactor. [12] A low pressure plasma (of the order of 0.1 mbar) was created by an rf discharge (13.56 MHz) between two parallel plate electrodes, 8 cm in diameter. The experimental arrangement consisting of the reactor, deposition control and vacuum pumps is shown in Fig. 1. Gas flows were controlled by electronic mass flow controllers. The total gas pressure was measured and automatically regulated through a butterfly valve by a Baratron pressure gauge. Crystalline silicon and Corning 7059 glass substrates were fixed on both electrodes. Depositions were made without additional heating of the substrate by a furnace, but due to heating by the plasma the temperature may rise to about 50°C.

The precursor gases were high purity hydrides,  $\text{H}_2\text{Se}$  and  $\text{GeH}_4$ . For the deposition of amorphous Se we used pure  $\text{H}_2\text{Se}$ , whereas for the rest of the compositions the gases  $\text{GeH}_4$  and  $\text{H}_2\text{Se}$  were diluted in hydrogen (15 vol.% of the hydrides). In order to get  $\text{Ge}_x\text{Se}_{1-x}$  samples of different chemical composition, three  $\text{GeH}_4/\text{H}_2\text{Se}$  gas ratios were used: 1/6, 1/12 and 1/24. The chemical composition of the  $\text{Ge}_x\text{Se}_{1-x}$  films deposited on the grounded electrode was determined by EDAX. X-ray diffraction showed that all the films were completely amorphous.

## 2.2. Determination of the optical constants by transmission measurements

First of all, the optical transmission spectra at normal incidence were obtained over the 300 to 2500 nm spectral region by a double-beam UV/vis/NIR computer-controlled spectrophotometer (Perkin-Elmer, model Lambda-19). The spectrophotometer was set with a slit width of 2 nm. The area of illumination over which a single transmission spectrum was obtained is about 1 mm × 10 mm. It should be stressed that the transmission spectra show that the PECVD  $\text{Ge}_x\text{Se}_{1-x}$  films have non-uniform thickness. This was confirmed by mechanical measurements of the film thickness with a stylus-based surface profiler (Sloan, Dektak model 3030). Fig. 2 shows a typical optical transmission spectrum of a  $\text{GeSe}_2$  film on a Corning 7059 glass substrate in the spectral range from the visible to the near infrared. A method first applied by Swanepoel [13] to inhomogeneous films of *a*-Si:H, and more recently by Márquez et al [14] to undoped and Ag-photodoped As-S glass films with non-uniform thickness, is used here to evaluate very accurately the optical constants, *n* and *k*, of the present PECVD Ge-Se films. Following this envelopes' method, we

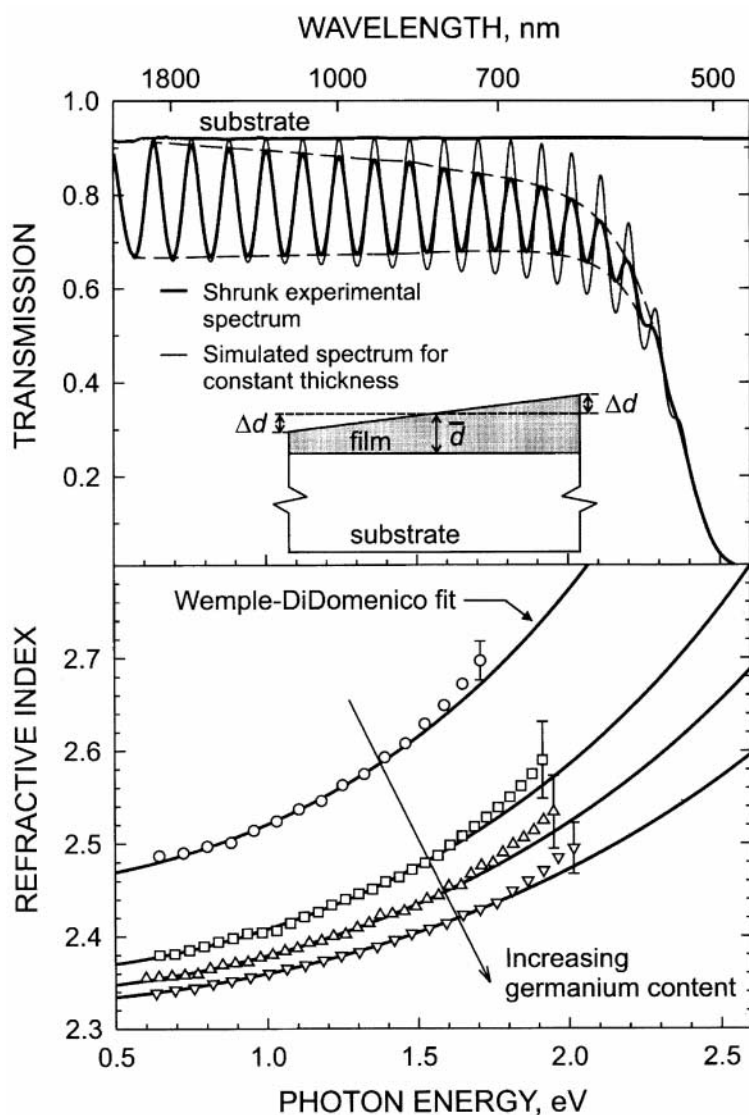


Fig. 2. A typical optical transmission spectrum of a non-uniform  $\text{GeSe}_2$  layer on a glass substrate, along with the corresponding envelopes, of the interference maxima and minima of the transmission spectrum; the inset shows a system of an absorbing thin film with a variation in thickness on a thick finite transparent substrate (in the particular case of the  $\text{GeSe}_2$  film,  $\bar{d} = 2095 \pm 23$  nm and  $\Delta d = 38 \pm 6$  nm). Also, the refractive index versus photon energy for various  $\text{Ge}_x\text{Se}_{1-x}$  films:  $\circ$ ,  $x = 0$ ;  $\square$ ,  $x = 0.17$ ;  $\triangle$ ,  $x = 0.25$ ;  $\nabla$ ,  $x = 0.34$ . Solid curves are determined according to the Wemple–DiDomenico single-oscillator analysis.

have also obtained the average thickness,  $\bar{d}$ , and the thickness variation,  $\Delta d$  (see Fig. 2).

### 3. Results and discussion

#### 3.1. Structural characterization

Although the germanium selenides have been intensively studied during the last fifteen years, the knowledge of their structure, especially of the Ge-rich and Se-rich alloys, is still clearly ambiguous. On the other hand, it is generally accepted that amorphous  $\text{GeSe}_2$  have a tetrahedral  $XY_4$ -type local structure. The structure of the amorphous germanium selenide films pre-

pared by PECVD has been already studied by Slecckx et al in [15, 16] using Raman spectroscopy. The typical Raman spectra of some of the present as-prepared PECVD films are represented in Fig. 3. Some relevant spectral features, regarding the structural consequences that can be derived from the optical measurements carried out in this work, are: in Se, a strong band at  $250 \text{ cm}^{-1}$ , attributed by Lucovsky [17] to stretching vibrations of Se atoms in helical chain-like and ring-like arrangements ('meandering chain'); in the Se-rich composition ( $x = 0.25$ ), a band near  $260 \text{ cm}^{-1}$  originating from Se–Se bonds, and a strong band at  $200 \text{ cm}^{-1}$  accompanied by a side band near  $215 \text{ cm}^{-1}$ , assigned to the stretching mode of  $\text{GeSe}_{4/2}$  corner-sharing tetrahedra ( $200 \text{ cm}^{-1}$ ) and to the vibrations of Se atoms in

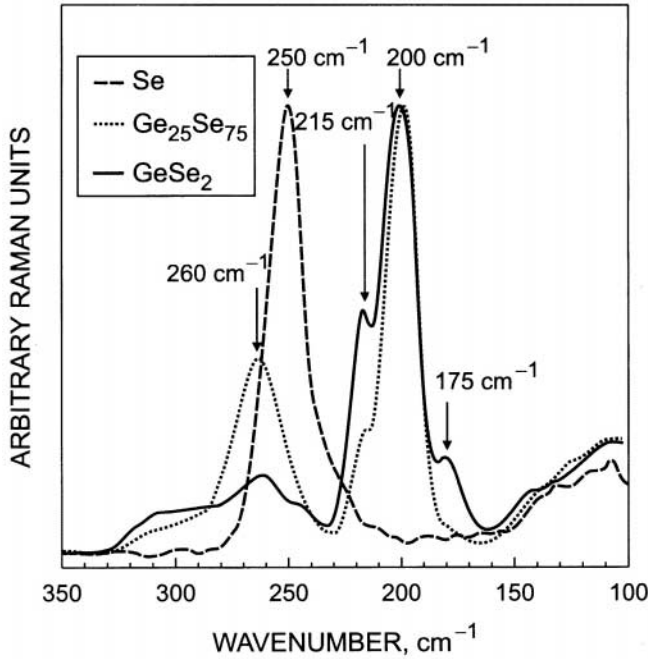


Fig. 3. Typical Raman spectra of as-deposited PECVD Ge–Se films.

four-membered rings composed of two edge-sharing tetrahedra ( $215\text{ cm}^{-1}$ ) [18]; in  $\text{GeSe}_2$ , in addition to the typical  $200\text{ cm}^{-1}$  band with its companion line, a small band at  $175\text{ cm}^{-1}$ , originating from Ge–Ge bonds, and the band at  $260\text{ cm}^{-1}$ , providing clear evidence for a structure containing Ge–Ge and Se–Se homopolar bonds in the stoichiometric material.

### 3.2. Dispersion behaviour of the refractive index

The final values of the refractive index for the PECVD  $\text{Ge}_x\text{Se}_{1-x}$  thin films under study are displayed in Fig. 2 as a function of the photon energy, and it can be observed that the values of the refractive index decrease notably with increasing germanium content; also, the value of the long-wavelength refractive index, i.e., the static refractive index,  $n(0)$ , which is determined using the optical dispersion relationship that will be introduced next, is listed in Table 1.

The data on the spectral dependence of the refractive index were evaluated according to the single-effective-oscillator model proposed by Wemple and

DiDomenico [19] and Wemple [20]. Those authors researched dispersion data for more than one hundred different materials, both covalent and ionic, and both crystalline and amorphous. They found that all the optical data can be described, to a very good approximation, by the following formula:

$$n^2(\hbar\omega) = 1 + \frac{E_d E_0}{E_0^2 - (\hbar\omega)^2} \quad (1)$$

where  $\hbar\omega$  is the photon energy,  $E_0$  is the oscillator energy and  $E_d$  is the oscillator strength or dispersion energy. Plotting  $(n^2 - 1)^{-1}$  against  $(\hbar\omega)^2$  allows one to determine the oscillator parameters by fitting a straight line to the points. The compositional dependence of the single-oscillator parameters is shown in Table 1: Both  $E_0$  and  $E_d$  increase with increasing Ge-content. The oscillator energy is an ‘average’ energy gap and to a reasonably good approximation it varies in proportion to the optical band gap, as was first found by Tanaka [21]. We will later compare the values of  $E_0$  listed in Table 1 with those of the optical gap,  $E_g^{\text{opt}}$ . Furthermore, the dispersion energy follows a simple empirical relationship,  $E_d = \beta N_c Z_a N_e$ , where  $\beta$  is a constant, and according to Wemple [20], for covalent crystalline and amorphous materials has a value of  $0.37 \pm 0.04\text{ eV}$ .  $N_c$  is the coordination number of the cation nearest neighbour to the anion,  $Z_a$  is the formal chemical valency of the anion and  $N_e$  is the effective number of valence electrons per anion. In the present case,  $Z_a = 2$ , and the corresponding values of  $N_e$  and  $N_c$  for the four compositions under analysis are listed in Table 1: It should be emphasized that the ‘natural’ coordination of each chemical element, that is, twofold and fourfold coordination for Se and Ge, respectively, has been approximately obtained from the present experimental values of the dispersion energy,  $E_d$ .

### 3.3. Optical-absorption edge and Tauc gap

The optical-absorption spectra derived by using the expressions corresponding to the envelope optical method for thin films with non-uniform thickness, proposed by Swanepoel, are displayed in Fig. 4 (it is clearly shown the remarkable blue-shift in the optical-absorption edge with increasing Ge-content).

Table 1. Values of the long-wavelength refractive index,  $n(0)$ , Wemple–DiDomenico gap,  $E_0$ , the dispersion energy,  $E_d$ , the effective number of valence electrons per anion,  $N_e = (4x + 6(1-x))/(1-x)$ , in the case of  $x \neq 0$ , the coordination number of the ‘cations’ surrounding an ‘anion’,  $N_c$ , the Tauc gap,  $E_g^{\text{opt}}$ , and the Tauc slope,  $B^{1/2}$ , for  $\text{Ge}_x\text{Se}_{1-x}$  films prepared by PECVD.

$x$	$n(0)$	$E_0$ (eV)	$E_d$ (eV)	$N_e$	$N_c$	$E_g^{\text{opt}}$	$B^{1/2}$ ( $\text{cm}^{-1/2}\text{ eV}^{-1/2}$ )
0	$2.453 \pm 0.002$	$3.97 \pm 0.05$	$19.92 \pm 0.23$	12.0	$2.24 \pm 0.04$	$1.93 \pm 0.02$	$1151 \pm 7$
0.17	$2.359 \pm 0.001$	$4.52 \pm 0.03$	$20.63 \pm 0.12$	6.8	$4.09 \pm 0.04$	$2.06 \pm 0.02$	$817 \pm 4$
0.25	$2.338 \pm 0.001$	$4.88 \pm 0.03$	$21.81 \pm 0.13$	7.3	$4.02 \pm 0.04$	$2.13 \pm 0.01$	$715 \pm 2$
0.34	$2.326 \pm 0.001$	$5.40 \pm 0.02$	$23.80 \pm 0.07$	8.1	$3.97 \pm 0.03$	$2.26 \pm 0.01$	$795 \pm 1$

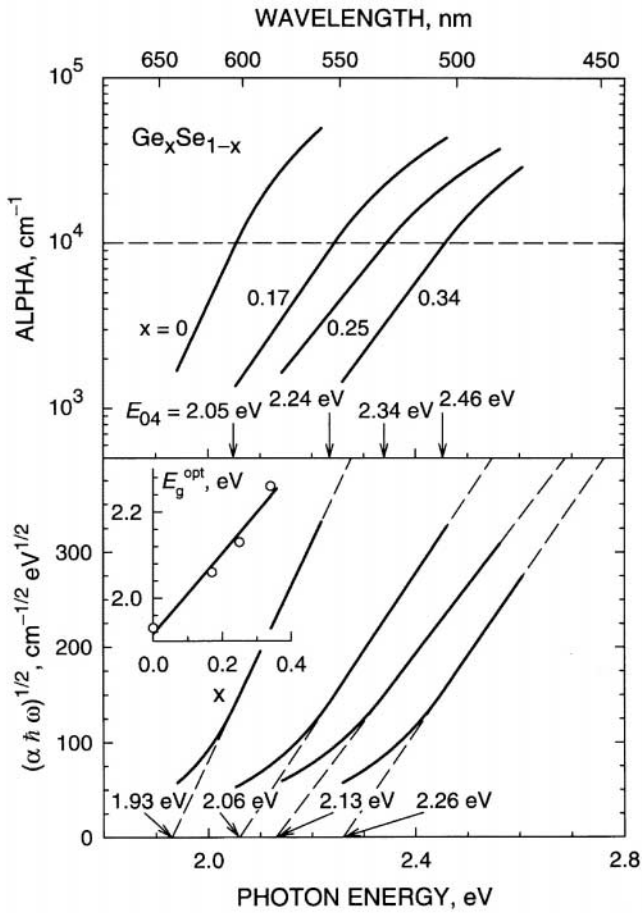


Fig. 4. Optical-absorption coefficient spectra for  $\text{Ge}_x\text{Se}_{1-x}$  films, with  $x = 0, 0.17, 0.25$  and  $0.34$  (the alternative, and very often used, optical gap,  $E_{04}$ , is defined as the energy where  $\alpha = 10^4 \text{ cm}^{-1}$ ). Furthermore, the plot of  $(\alpha\hbar\omega)^{1/2}$  versus  $\hbar\omega$  (Tauc's extrapolation) for the PECVD films under study. The inset displays one of the three gaps reported in this paper,  $E_g^{\text{opt}}$ , versus germanium content for all the thin-film samples.

Continuing with the analysis of the optical absorption, the optical band gap is now introduced. It is defined according to the 'non-direct transition' model proposed by Tauc [22], as the intersection of the straight line through the high-energy points of a graph of  $(\alpha\hbar\omega)^{1/2}$  versus  $\hbar\omega$ , with the energy axis (see Fig. 4). This implies

$$(\alpha\hbar\omega)^{1/2} = B^{1/2}(\hbar\omega - E_g^{\text{opt}}) \quad (2)$$

where  $B^{1/2}$  is the so-called Tauc slope. This relationship assumes that the densities of electron states in the valence and conduction bands near the band gap have a parabolic distribution and, also, that the matrix elements for the interband transitions associated with the photon absorption, are equal for all transitions. The dependences of  $E_g^{\text{opt}}$  and  $B^{1/2}$  on the Ge-content in PECVD  $\text{Ge}_x\text{Se}_{1-x}$  films are shown in Table 1: The Tauc gap increases linearly (see Fig. 4) and the Tauc slope decreases remarkably with increasing Ge-content

(it is worth noting that the values of  $E_g^{\text{opt}}$  are in excellent agreement ( $< 3\%$ ) with those previously calculated using another optical procedure, based on both transmission and reflection measurements [16]). Interestingly, the value of the Tauc gap of a representative thermally-evaporated  $a\text{-GeSe}_2$  film, 2.06 eV, is much lower than that of the corresponding PECVD film, the difference being due to the incorporation of hydrogen in the plasma-deposited films, detected in the Raman spectra (this was clearly evidenced by the presence of a Raman band at  $2240 \text{ cm}^{-1}$ , arising from Se–H vibrations [16]). On the other hand, going back to the Wemple–DiDomenico gap,  $E_0$ , it verifies fairly well the relationship  $E_0 \approx 2 \times E_g^{\text{opt}}$  (although, rather surprisingly, it increases slightly with increasing Ge-content). In order to complete the computation of the optical constants, the extinction coefficient,  $k$ , is easily determined from the  $\alpha$ -values, using the formula,  $k = \alpha\lambda/4\pi$ . Also, Fig. 2 shows the simulated transmission spectrum (obtained using the calculated values of  $n$  and  $k$  [23]) corresponding to a  $\text{GeSe}_2$  film of constant thickness, equal to the average thickness ( $2095 \pm 23 \text{ nm}$ ) of the representative  $\text{GeSe}_2$  film under analysis.

Finally, the specific optical properties of the Se-rich  $\text{Ge}_x\text{Se}_{1-x}$  films, i.e., the decrease of the refractive index and the corresponding increase of the Tauc gap with increasing Ge-content could be explained if the Ge–Se binary system is regarded as a network of covalently bonded germanium atoms (as it was previously mentioned, coordination number = 4) and selenium atoms (coordination number = 2), and if the optical constants are strongly related to several chemical bond types (Ge–Ge, Se–Se and Ge–Se) and their relative number, following the ideas first suggested by Lucovsky [1] and more recently by Broese *et al.* [6].

#### 4. Conclusions

We have demonstrated that PECVD is an efficient and promising film preparation method; the composition range which can be achieved by this technique is very broad. Raman measurements are suitable for determining the local structure of these particular amorphous chalcogenides. From optical transmission experiments we were able to derive very accurately (with an accuracy better than 2%) the optical constants in the visible and near infrared range of the plasma-deposited non-uniform  $\text{Ge}_x\text{Se}_{1-x}$  thin films, with  $x = 0, 0.17, 0.25$  and  $0.34$ . A detailed analysis of the refractive-index dispersion based on the Wemple–DiDomenico single-oscillator framework allows us to gain further information on the structure of the films. The optical gaps,  $E_g^{\text{opt}}$ , were all of them calculated

using Tauc's extrapolation, resulting in values ranging from 1.93 eV for pure *a*-Se up to 2.26 eV for *a*-GeSe<sub>2</sub>.

## References

- [1] Lucovsky G. Phys. Rev. B 1977;15:5762.
- [2] Burckhardt W, Feltz A. Phys. Status Solidi (a) 1983;80:463.
- [3] Butterfield AW. Thin Solid Films 1974;23:191.
- [4] Kotkata MF, Kandil KM, Thèye ML. J. Non-Cryst. Solids 1993;164-166:1259.
- [5] Ruíz-Pérez J, Márquez E, Minkov D, Reyes J, Ramírez-Malo JB, Villares P, Jiménez-Garay R. Phys. Scripta 1996;53:76.
- [6] Broese E, Schröter B, Lehmann A, Richter W, Schirmer G. J. Non-Cryst. Solids 1991;130:52.
- [7] Choi J, Singh A, Davis EA, Gurman SJ. J. Non-Cryst. Solids 1996;198-200:680.
- [8] Fritzsche H, Smíd V, Ugur H, Gaczi PJ. J. Phys. (Paris) 1981;10:C4-699.
- [9] Nagels P, Callaerts R, Van Roy M, Vlcek MJ. Non-Cryst. Solids 1991;136-137:1001.
- [10] Nagels P. Electronic, Optoelectronic and Magnetic Thin Films, Marshall JM, Kirov N, Vavrek A, editors. Research Studies, Taunton, Somerset, 1995, p. 262.
- [11] Cardinaud C, Turban G, Cros B, Ribes M. Thin Solid Films 1991;205:165.
- [12] Sleenckx E, Nagels P, Callaerts R, Van Roy M. J. Phys. IV 1993;3:C3-419.
- [13] Swanepoel R. J. Phys. E: Sci. Instrum. 1984;17:896.
- [14] Márquez E, Ramírez-Malo JB, Fernández-Peña J, Villares P, Jiménez-Garay R, Ewen PJS, Owen AE. J. Non-Cryst. Solids 1993;164-166:1223.
- [15] Sleenckx E, Nagels P, Callaerts R, Van Roy M. J. Non-Cryst. Solids 1993;164-166:1195.
- [16] Sleenckx E, Tichy L, Nagels P, Callaerts R. J. Non-Cryst. Solids 1996;198-200:723.
- [17] Lucovsky G. The Physics of Selenium and Tellurium. Berlin: Springer, 1979, p. 210.
- [18] Sugai S. Phys. Rev. B 1987;35:1345.
- [19] Wemple SH, DiDomenico M. Phys. Rev. B 1971;3:1338.
- [20] Wemple SH. Phys. Rev. B 1973;7:3767.
- [21] Tanaka K. Thin Solid Films 1980;66:271.
- [22] Tauc J. Amorphous and Liquid Semiconductors. New York: Plenum Press, 1974, p. 159.
- [23] Heavens OS. Optical Properties of Thin Solid Films. London: Butterworths, 1955, p. 77.